

Tidal modulation of wave-setup and wave-induced currents on the Aboré coral reef, New Caledonia.

P. Bonneton[†], J-P. Lefebvre[‡], P. Bretel[†], S. Ouillon[‡] and P. Douillet[‡]

[†] Department of Geology and Oceanography
UMR EPOC
University of Bordeaux I
Avenue des Facultés
33405 Talence, France

[‡] Centre IRD Nouméa
BP A5
98848 Nouméa
New Caledonia

p.bonneton@epoc.u-bordeaux1.fr



ABSTRACT

BONNETON, P., LEFEBVRE, J-P., BRETTEL, P., OUILLOIN, S. and DOUILLET, P., 2007. Tidal modulation of wave-setup and wave-induced currents on the Aboré coral reef, New Caledonia. *Journal of Coastal Research*, SI 50 (Proceedings of the 9th International Coastal Symposium), 762 – 766. Gold Coast, Australia, ISSN 0749.0208

As waves break on a reef, they create a radiation stress gradient that drives wave-setup and wave-induced currents. In this paper, tidally modulated wave-induced current and wave-setup are presented and analysed from field measurements performed on the Aboré coral reef in the southwest lagoon of New Caledonia. We show, in agreement with analytical models by Symonds et al (1995) and Hearn (1999), that this tidally modulated wave circulation is mainly controlled by the difference between the depth at the breakpoint and the water depth over the reef. A specific calibration of these models is proposed for the Aboré reef.

ADDITIONAL INDEX WORDS: *wave breaking, surf zone, lagoon, coral reef*

INTRODUCTION

As waves break on a reef, they create a radiation stress gradient that drives wave-setup and wave-induced currents (e.g. Tait (1972), Symonds et al. (1995), Hearn (1999) or Gourlay and Colleter (2005)). These phenomena exert a major influence on the hydrodynamics, morphology and biological variability of shallow submerged coral reefs and have a significant impact on the circulation and flushing of lagoons.

An ongoing integrated study of the southwest lagoon of New Caledonia investigates the space-time variability of its physical, chemical, biological and sedimentological parameters. It aims at assessing the impact of human activities on marine ecosystems and is based on field measurements and modelling (see Jouon et al. (2006)). A 3D model of hydrodynamics and particle transport was adapted to this site (Douillet et al. (2001)), but the exchanges between the ocean and the lagoon above the barrier reef are only schematic in the model and need to be improved. Therefore, it seems important to characterise wave-setup and wave-induced flows over the New Caledonia reef.

In this area, the tides are semidiurnal with a tidal range on the reef varying from about 1.4 m at spring to 0.6 m at neap (Douillet (1998)). The tidal evolution of water depth over the reef top has a strong influence on the wave-induced phenomena (see Gourlay and Colleter (2005) and Andréfouët et al. (2006)). However, only few field experiments have been devoted to the analysis of both tidally modulated wave-induced current (e.g. Tartinville and Rancher (2000)) and tidally modulated wave-setup.

To understand the dynamics of these phenomena over the New Caledonia reef, a field experiment was conducted on the Aboré coral reef (southwest lagoon of New Caledonia) in October 2005.

In this paper, we present the first analysis of the data acquired during the experiment. In particular we show, in agreement with analytical models by Symonds et al (1995) and Hearn (1999), that tidally modulated wave setup and wave-induced current on the Aboré reef are mainly controlled by the difference between the depth at the breakpoint and the water depth over the reef.

MATERIALS AND METHODS

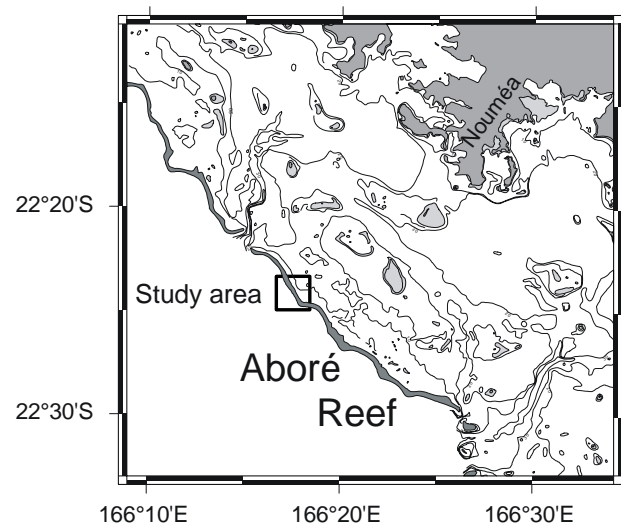


Figure 1. The study area in the southwest lagoon of New Caledonia

Study area

New Caledonia is located 1,500 km eastward of Australia at the southern end of the Melanesian Arc. The lagoons cover a total area of 23,400 km². The southwest part of these lagoons (Figure 1), which is delimited by a barrier reef and the island coast, is approximately 20 km wide with an average depth of 17.5 m. Tides, currents and sediment transport have been extensively studied within the southwest lagoon (see Jouon et al. (2006)). Deep passes bisect the barrier reef and the reef crest is exposed at spring low tide. The studied site lies in the northern part of the Aboré reef (figure 1). In order to minimise the influence of both wave refraction and strong tidal currents in the passes, the location was chosen in a rather straight section of the reef perpendicular to the dominant oceanic wave direction and far from the passes.

At the chosen location, the reef is constituted by a reef flat of about 120 m width bordered by a seashore slope β of 1/10 and separated from the lagoon by a step of about 1 m (figure 2). The height of the reef flat is evaluated to be 0.10 m above the lowest tide level during mean spring tide. Living corals mostly colonise the outer rim of the reef and the reef flat is dominated by rubbles and boulders.

Instruments

In order to achieve measurements all along the cross-shore propagation of the waves, a set of sensors was deployed along a transect (Figure 2). Tidal level evolution and incident wave characteristics were measured at 2-Hz sample rate by a non-directional Wave and Tide Recorder (WTR 9, Aanderaa). This instrument was deployed on the external reef slope (site A_o in figure 2), in a mean water depth of 6.5 m. On the reef flat, two sets of an acoustic Doppler velocimeter (ADV Vector, Nortek) coupled with two pressure sensors (26W, Keller) were deployed, one near the external reef rim (sites P1,2 and adv1 in Figure 2) and

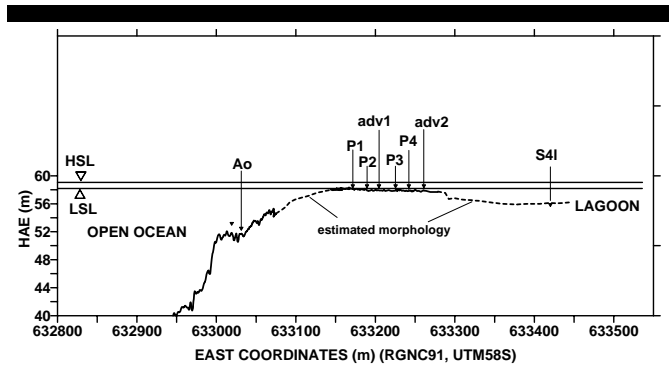


Figure 2. Reef profile and instruments deployment. P1-4: 0-2 bar absolute pressure sensors; adv1-2: acoustic doppler velocimeters; S4i: electromagnetic current meter; A_o: non-directional wave and tide recorder. HSL: highest measured sea level, LSL: lowest measured sea level. HAE: Height Above Ellipsoid IAG GRS80.

the other near the inner edge of the reef (sites P3,4 and adv2 in Figure 2). For each set, the pressure sensors were regularly spaced every 20 m. All measurements on the reef flat were sampled synchronously at a frequency of 8 Hz. These (high-frequency) data allow us to investigate processes, such as oscillating bores or infragravity waves propagating over the reef top. However, the present paper is mainly focused on the analysis of the complex (low-frequency) tidal influence on both wave-setup and wave-induced currents.

In order to characterise wave-induced currents and residual wave signal after its propagation across the reef, an S4 InterOcean electromagnetic current meter was deployed at the inner end of the transect, about 150 m from the reef edge, in a mean water depth of

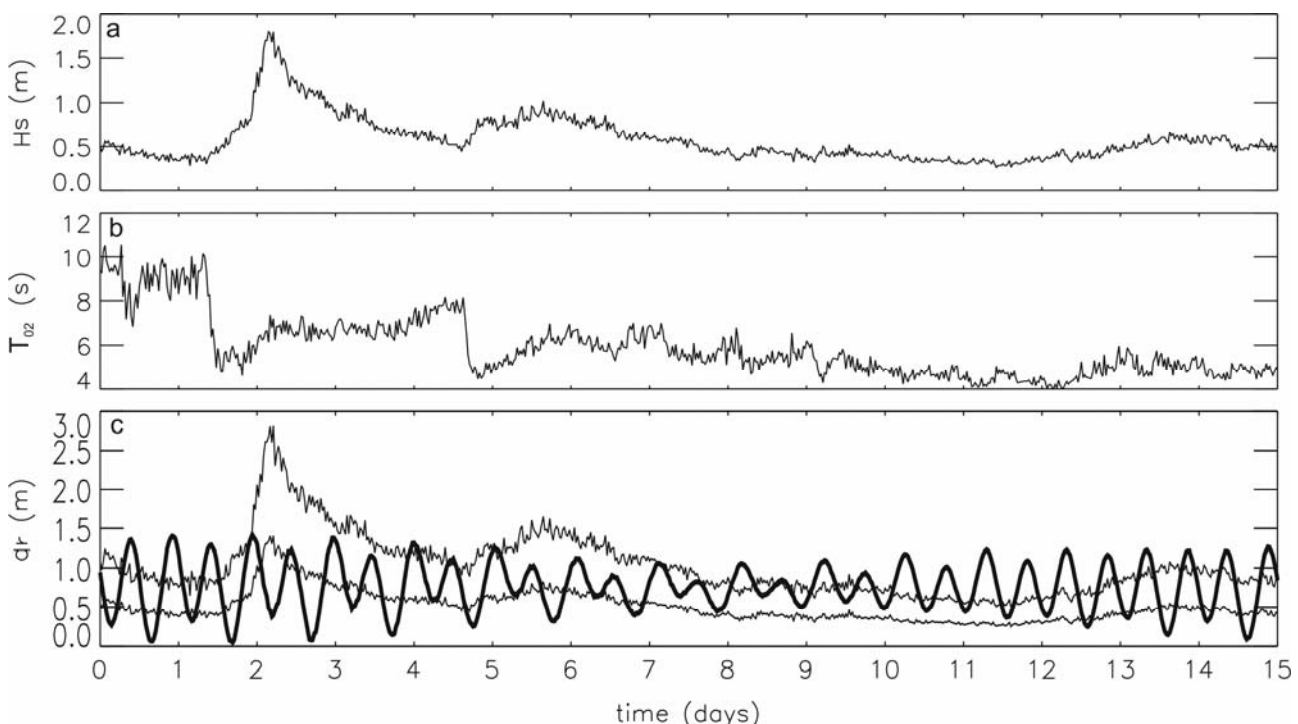


Figure 3. Wave and tide conditions. (a) incident significant wave height in a 6.5 m mean water depth; (b) incident wave period; (c) bold line: 30-minute averaged water depth at the reef top d_r , thin lines: h_b and $h_b/2$, where h_b is the breakpoint water depth.

3m (site S4₁ in fig. 2). Data were continuously acquired at a 2-Hz sample rate.

The topography of the study area, presented in figure 2, was acquired by use of a DGPS (Trimble 5700), with a vertical accuracy of 5 cm.

Pressure measurements, corrected from atmospheric variations, were converted to water depth, and knowing the topography elevation Z , to sea surface elevation ζ . The reef-top wave setup ζ_r is given by $\zeta_r = \zeta_{P1} - \zeta_{A_0}$, where ζ_{P1} and ζ_{A_0} are the 30-minute averaged elevations measured respectively at P1 (on the reef top) and A₀ (offshore conditions). The setup variations are accurately measured but, mainly due to Z -inaccuracy, the absolute error for ζ_r is about 5 cm.

Sea-state conditions

The experiment was conducted from the 18th October (day 0) to 2nd November, 2005 (day 15). Time series of incident significant wave height H_s and wave period T_{02} are presented in figures 3a and 3b. We can schematically distinguish two main sea-state conditions. For the first one, from day 0 to day 7, the wind speed was weak (about 5 m/s) and was predominant from the west-northwest. The sea-state conditions were dominated by westerly waves propagating nearly normally to the reef, with H ranging from 0.3 to 1.8 m and T_{02} ranging from 5 to 10 s. For the second regime, from day 7 to day 15, the offshore wave field corresponded to south-easterly wind wave of weak intensity ($H_s \in [0.25 \text{ m}, 0.65 \text{ m}]$) and short period ($T_{02} \in [4 \text{ s}, 6 \text{ s}]$). These waves were associated to south-easterly trade winds of about 10 m/s. During this second regime the wave field on the reef was very complex because low-energy wind waves were propagating both from offshore and from the lagoon. Consequently, in this paper our analysis of wave-induced circulation on the reef will be mainly based on data acquired during the first sea-state regime.

Time series of mean water depth over the reef-top, $d_r = \zeta_{A_0} - Z_r$ (ζ_{A_0} : 30-minute averaged sea elevation measured in site A₀; Z_r : reef-top elevation) shows strong semi-diurnal oscillations. During the whole experiment d_r ranged from 5 to 140 cm.

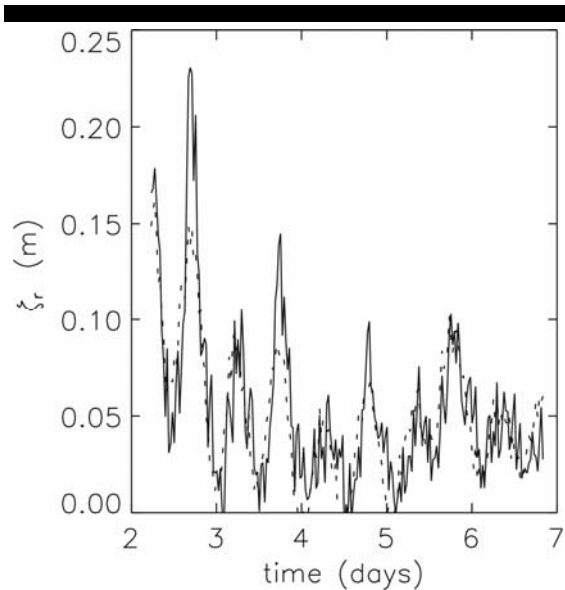


Figure 4. Comparison between observed (solid line) and calculated (dashed line, eq. 1) wave setup ζ_r on the reef-top.

RESULTS

Time evolution, during the first sea-state regime, of the reef-top wave setup, ζ_r , is presented in Figure 4. We observe that ζ_r evolution is strongly correlated to tidal level oscillations. Figures 4 and 3 show that ζ_r oscillates 180° out of phase with the water depth over the reef-top d_r . These figures also show that for a fixed d_r -value the wave setup is an increasing function of the incident wave height.

The time series of cross-reef currents measured on the reef-top, at site adv1, and in the lagoon, at site S4₁, are presented in Figure 5. During the experiment, the cross-reef current was an order of magnitude higher than its along-reef component. The time series of cross-reef current at the reef top, u_r , is discontinuous

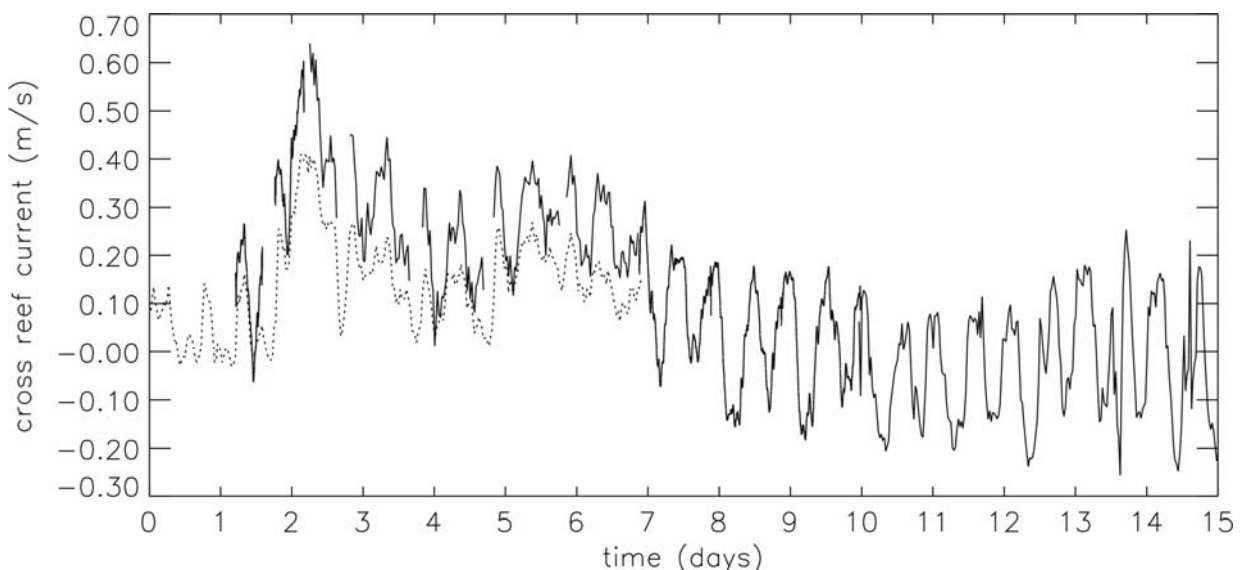


Figure 5. Thirty minute averaged cross reef currents measured on the reef-top at site adv1 (solid line) and in the lagoon at site S4₁ (dashed line).

because the avd1 current metre was exposed at some low tides. For the first sea-state regime (from days 0 to 7) cross-reef currents were mainly positive (i.e. lagoonward directed) and u_r reached a maximum value of 0.65 m/s. Figures 5 and 3a show that cross-reef currents increase as the significant wave height increases. The cross-reef currents oscillate at twice the tidal frequency, with maximum values occurring around mid-tides. This observation is more visible with the continuous S4₁ data series (dashed line). All these results show that the observed reef currents were mainly controlled by the process of wave-induced currents. However, it is clear that cross-reef currents are higher during rising tide than falling tide. This shows that if cross reef currents are mainly composed of a tidally modulated wave-induced current, they included also a true tidal current component.

For the second sea-state regime (from days 7 to 15), which

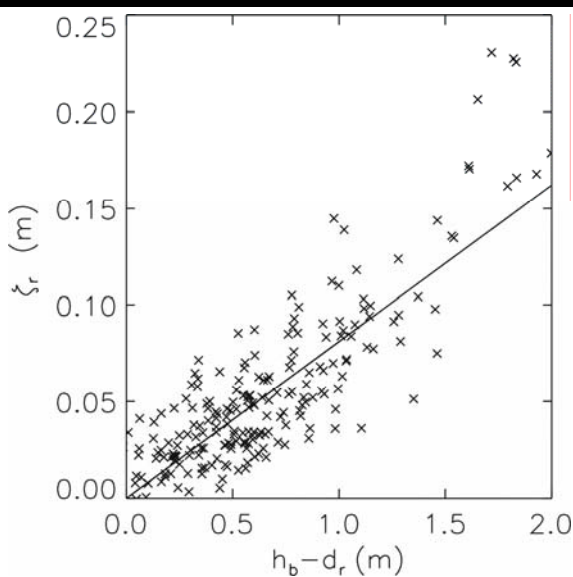


Figure 6. Wave setup on the reef-top, ζ_r , as a function of $h_b - d_r$, from data acquired between day 2 and day 7. The solid line is a least squares best fit, $\zeta_r = 0.081(h_b - d_r)$, with a correlation coefficient of 0.83.

corresponded to a complex low energy wind wave field, currents show a different evolution. Indeed, u_r oscillated around zero at the tidal frequency, 180° out of phase with the water depth d_r . The cross-reef current was maximum (lagoonward directed) at low tide and minimum (seaward directed) at high tide.

DISCUSSION

Symonds et al. (1995) and Hearn (1999) have derived models which provide simple analytical formulations of ζ_r and u_r as a function of reef geometry characteristics and incident wave forcing, defined by the depth at the breakpoint h_b and the water depth over the reef d_r . In this section we analyse the ability of these models to reproduce the tidal modulation of wave-setup and wave-induced currents described in the preceding section.

For the Aboré reef, the parameter $(\beta x_L)/d_r$, where β is the reef slope and x_L the reef flat width, is large in comparison with 1. In that case, Symonds et al.'s model can be reduced to equations:

$$\zeta_r = \alpha(h_b - d_r) \quad (1)$$

$$u_r = K_S d_r (h_b - d_r) \quad (2)$$

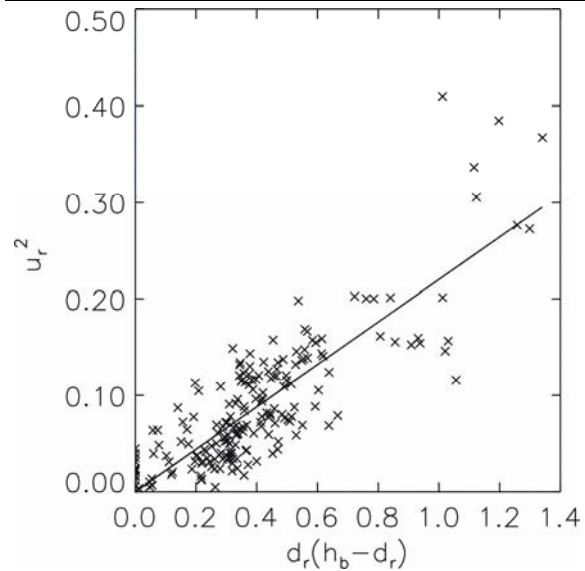


Figure 7. Square of the cross reef current u_r , as a function of $d_r(h_b - d_r)$, from data acquired between day 2 and day 7. The solid line is a least squares best fit, $u_r^2 = 0.22d_r(h_b - d_r)$, with a correlation coefficient of 0.83.

if $h_b \geq d_r$, where α is a dimensionless coefficient and K_S is a parameter related to reef geometry and bottom friction. $\zeta_r = 0$ and $u_r = 0$ if $h_b < d_r$. Assuming that $\zeta_r/d_r \ll 1$, Hearn's model leads to an expression similar to equation (1) for the setup and to the cross-reef current equation:

$$u_r^2 = K_H d_r (h_b - d_r) \quad (3)$$

To compare these formulations to the experimental data presented in figures 4 and 5, h_b is computed using linear shoaling theory combined with the breaking criteria given by Symonds et al. (1995) : $H_{sb}/h_b = 0.7$. The computed time series of h_b is shown in figure 3c. Wave setup data, presented in figure 4, are plotted against $h_b - d_r$ in figure 6. The data points are well fitted by a linear regression in agreement with equation (1). Figure 4 shows, that with the best-fit coefficient $\alpha = 0.081$, equation (1) gives a good description of the tidally modulated wave setup evolution.

For the cross-reef current data, we find a good correlation between u_r and $d_r(h_b - d_r)$, but which does not follow a linear regression. On the other hand, u_r^2 data plotted against $d_r(h_b - d_r)$ in Figure 7, show that the data points are well fitted by a linear regression, in agreement with Hearn's model. We can see in Figure 8 that equation (3), with the best-fit parameter $K_H = 0.22 \text{ s}^{-2}$, gives a good description of the tidal modulation of wave-induced current at twice the tidal frequency.

From equation (3), we can deduce that, for given wave conditions, the maximum cross-reef current is reached for $d_r = h_b/2$. The time series of h_b , $h_b/2$ and d_r are shown in figure 3c. In this figure we can see that for the first sea-state regime (days 0 to 7) the condition $d_r = h_b/2$ is generally reached twice a tide. This is in agreement with the observations (Figures 5 and 8) of a maximum cross-reef current twice a tide. On the opposite, for the second sea-state regime (days 7 to 15), $h_b/2$ is generally smaller than d_r , which implies from equation (3) that u_r is a decreasing function of d_r . This analysis is consistent with the observations (Figure 5) which show that u_r oscillated at the tidal frequency, 180° out of phase with the water depth d_r .

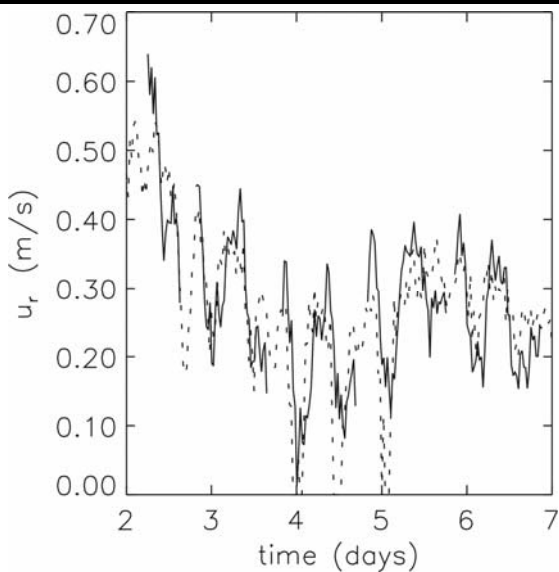


Figure 8. Comparison between observed (solid line) and calculated (dashed line, eq. 3) cross reef current on the reef-top u_r .

CONCLUSION

Field measurements on the Aboré reef of New Caledonia show that the average crossshore current on the reef flat is always directed towards the interior of the lagoon when energetic ocean waves propagate quasi perpendicularly towards the Aboré Reef. In this case, the current is thus primarily generated by the swell and not by the tide. Models suggested by Symonds et al. (1995) and Hearn (1999), which quantify the current on the reef according to the swell and the tide, were validated and calibrated at the study site from parameters integrated over the wave period. Additional field campaigns at other sites may be aimed at studying the sensitivity of these coefficients to reef geometry and bottom friction. A generalisation of the mathematical formulations to the whole of the barrier reef will make it possible to estimate, by using swell data provided by altimetry, the total flows generated by the swell in the south-west lagoon of New Caledonia. In the medium term, these models will be introduced into the 3D hydro-sedimentary model of the southwest lagoon of New Caledonia (Douillet et al. (2001)).

Except from the quantification of average quantities (integrated over the period of the waves) such as the “set-up” or the oceanic inputs induced by wave breaking, the measurements also will enable us to better understand “high frequency” dynamics of waves over the reef flat. For example, we have observed that turbulent bores propagating over the reef flat evolve into oscillating bores. This physical process controls wave energy dissipation and thus plays an important role in wave-induced circulation. Such a process of wave transformation on the reef will be presented in a future paper.

LITERATURE CITED

ANDRÉFOUËT, S., OUILLO, S., BRINKMAN, R., FALTER, J., DOUILLET, P., WOLKE, F., SMITH, R., GAREN, P., MARTINEZ, E., LAURENT, V., LO, C., REMOISSENET, G., SCOURZIC, B., GILBERT, A., DELEERSNIJDER, E., STEINBERG, C., CHOUKROUN, S. and BUESTEL D., 2006. Review of solutions for 3D hydrodynamic modelling applied to aquaculture in South

Pacific atoll lagoons, *Marine Pollution Bulletin*, 52, 1138-1155.

DOUILLET, P., 1998. Tidal dynamics of the south-west lagoon of New Caledonia: observations and 2D numerical modelling. *Oceanologica Acta*, 21, n°1, 69-79.

DOUILLET, P., OUILLO, S. and CORDIER, E., 2001. A numerical model for fine suspended sediment transport in the south-west lagoon of New-Caledonia, *Coral Reefs*, 20, 361-372.

GOURLAY, M.R. and COLLETER, G., 2005. Wave-generated flow on coral reefs – an analysis for two-dimensional horizontal reef-tops with steep faces. *Coastal Engineering*, 52, 353-387.

HEARN, C.J., 1999. Wave-breaking hydrodynamics within coral reef systems and the effect of changing relative sea level. *Journal of Geophysical Research*, 104, C12, 30,007-30,019.

JOON, A., DOUILLET, P., OUILLO, S. and FRAUNIE, P., 2006. Calculations of hydrodynamic time parameters in a semi-opened coastal zone using a 3D hydrodynamic model, *Continental Shelf Research*, 26, 1395-1415.

SYMONDS, G., BLACK, K.P. and YOUNG, I. R., 1995. Wave-driven flow over shallow reefs. *Journal of Geophysical Research*, 100, C2, 2639-2648.

TAIT, R.J., 1972. Wave set-up on coral reefs. *Journal of Geophysical Research*, 77, 2207-2211.

TARTINVILLE, B. and RANCHER, J., 2000. Wave-induced flow over Mururoa atoll reef. *Journal of Coastal Research*, 16, n°3, 776-781.

ACKNOWLEDGEMENTS

This study was performed within the framework of the French scientific program PNEC (Programme National Environnement Côtier). The authors thank Guillaume Dirberg and Jean-Pierre Lamoureux for their contributions.